

SUPPLEMENTARY INFORMATION

Nanoparticle binding attenuates the pathobiology of gastric cancer-associated *Helicobacter pylori*

Dana Westmeier^{1,*}, Gernot Posselt², Angelina Hahlbrock¹, Sina Bartfeld³, Cecilia Vallet⁴, Carmen
5 Abfalter², Dominic Docter¹, Shirley K. Knauer⁴, Silja Wessler², and Roland H. Stauber^{1*}

*Corresponding author: Roland H. Stauber, roland.stauber@unimedizin-mainz.de; Dana Westmeier, danawestmeier@uni-mainz.de

10 Table of Contents

		page
	SUPPLEMENTARY METHODS	
	Nanoparticle synthesis and characterization.	S3
	Bacterial cultivation.	S3
15	NP-bacteria complex formation and characterization.	S4
	Protein separation by 1-D gel electrophoresis.	S4
	Cells, cell culture and toxicity assays.	S5
	Immunoblotting.	S5
	Fluorescence microscopy.	S5
20	Scanning electron microscopy (SEM).	S6
	Atomic force microscopy (AFM).	S6
	Energy dispersive X-Ray spectroscopy (EDX).	S7
	Quantification of bacteria internalization in human cells by automated microscopy.	S7
	PCR.	S7
25	Human Tissue Material.	S8
	Organoid culture and infection.	S8
	Reagents.	S9
	Statistical Analysis.	S9
30	SUPPLEMENTARY TABLES	
	S1 EDX analysis.	S10
	S2 Gastric fluid simulation media.	S10
	SUPPLEMENTARY FIGURES	
35	S1 Investigation of NP-bacteria complex formation.	S11
	S2 Calculation of maximal surface occupation by NPs	S12
	S3 Physico-chemical characteristics of NPs are critical for complex formation with bacteria.	S13
	S4 NP-bacteria complex formation is pH-dependently enhanced.	S14
40	S5 Impact of the biomolecule corona on NP-bacteria complex formation.	S15
	S6 Enhanced binding of NPs to bacteria improves the antibacterial activity of the NPs.	S16
	S7 Bacterial viability was not affected by Si30 even when high concentrations were used.	S17

S8 Impact of NP-pathogen complex formation.

S18

SUPPLEMENTARY REFERENCES

S19

SUPPLEMENTARY METHODS

Nanoparticle synthesis and characterization. Blue (AF350), red (rhodamine B) or green (FITC) fluorescent as well as non-fluorescent amorphous NPs (Si) of different sizes, modified by different surface-functionalization (amine, carboxylate, and unmodified) were purchased from (MainzScreeningCenterUG&CoKG) and used as described.(1, 2) Carbon black (CAS#1333-86-4) was purchased from Sigma Aldrich. ZnO NPs were provided by the DENANA research consortium and prepared by flame spray pyrolysis as described.(3) Non-coated positively and negatively charged fluorescent (rhodamine B) poly(organosiloxane) NPs (POSi) modified by different surface-functionalization, such as poly(ethylene glycol) (PEG) or poly(2-ethyl-2-oxazoline), were synthesized and used as described.(4) Briefly, carboxy-functionalized NPs (POSi_{RC}) were obtained by polycondensation of different alkoxysilanes in aqueous dispersion. Positively charged NPs (POSi_{RN}) were synthesized by coupling of *N,N*-diethylethylethylendiamine. PEGylated NPs (POSi_{RPEG}) were prepared by adding PEG to maleimido-functionalized NPs. For synthesis of poly(2-ethyl-2-oxazoline)-modified NPs (POSi_{RPEIO}), poly(2-ethyl-2-oxazoline) was reacted with maleimido-functionalized NPs according to.(4) NPs were characterized by TEM, SEM, AFM, DLS, and zeta potential measurements as reported.(1, 2) Briefly, transmission electron microscopy (TEM) imaging was performed using a Philips EM420 on carbon coated copper grids. The size and zeta potential were determined with a Malvern Zetasizer NanoZS as described.(5) Average particle size as well as size distribution was determined by dynamic light scattering (DLS) using a Nicomp380 Submicrometer Particle Sizer (Nicomp Particle Sizing Systems) at 20°C operating at a scattering angle of 90°. DLS results are reported as the average of at least 3 runs, each containing 100 individual measurements.

Bacterial cultivation.

For fluorescence microscopy experiments, genetically modified bacteria strains were used expressing red fluorescent protein tdTomato (^(p)*gpdA::dTomato::his2A^(t)* <*ptrA*> (here *E. coli*^{RFP}) or (^(p)*gpdA::EGFP::his2A^(t)* <*ptrA*> expressing green fluorescent protein GFP (here *E. coli*^{GFP}, *H. pylori*^{GFP}). *E.coli*^{GFP/RFP} were grown in LB medium with 100 µg/mL Ampicillin. *H. pylori* strain P12 (wild type; expressing Western CagA EPIYA-ABCC) has been described previously.(6) *H. pylori*^{GFP} were cultured in BHI medium (37 g/L brain heart

infusion) with 6 µg/mL Chloramphenicol and 10 g/L Cyclodextrin under microaerophilic conditions.

NP-bacteria complex formation and characterization. Bacteria concentrations were determined using the Cell Counter Casy I-TT (Innovatis AG). Bacteria were washed five times before incubation with NPs in the indicated media, temperature, and time points. NP-bacteria complexes were harvested by mild centrifugation (10 min, 3,000 rpm, 20 °C), the pellet was resuspended in PBS buffer and another washing step (10 min, 3,000 rpm, 20°C) was performed before resuspension in PBS buffer. NP-bacteria complex formation was performed based on the calculation of theoretical NP-bacteria binding. The surface area of a single bacterium is $\sim 13.5 \mu\text{m}^2$ (assuming ideal cylinder with hemispheres at both ends). The maximum area occupied by NPs (Si_{30} ; $\varnothing \sim 30 \text{ nm}$) corresponds to their cross-sectional area of $\sim 706.9 \text{ nm}^2$. Hence, it is estimated that maximally $\sim 2 \times 10^4$ NP (Si_{30} ; $\varnothing \sim 30 \text{ nm}$) can bind to a single bacterium. Interaction studies at different pH were performed in: 1 M NaOAc (pH 3), 1 M NaOAc (pH 5) and 1x Tris HCl (pH8). Gastric fluid simulation media was prepared according to Supplementary Table S2. For cell culture experiments, a NP coverage of the bacterial surface of 25 or 0.25 % was used for the formation of bacteria/NP complexes. As cells were exposed at a MOI of ~ 5 , the maximum Si_{30} NP dose/cell is estimated to be $\sim 2.5 \times 10^2$ ng, assuming that all bacteria are coming into contact with the cell. SEM data showed that even incubation with the maximum number of NP theoretically fitting onto the surface of a single bacterium resulted in a surface coverage of only $\sim 60\text{-}80\%$. Thus, we assume that $\sim 1.5 \times 10^3$ Si_{30} NP are attached per bacterium.

Cells, cell culture and toxicity assays. Authenticated and characterized cell lines were purchase from the ATCC repository, expanded, stocks prepared at early passages, and frozen stocks kept in liquid nitrogen. Thawed cells were routinely monitored by visual inspection and growth-curve analyzes to keep track of cell-doubling times, and were used for a maximum of 20 passages for all experiments. Depending on passage number from purchase, cell line authentication was further performed at reasonable intervals by short tandem repeat (STR) profiling. Caco-2 cells (ATCC HTB-37) and THP-1 cells (ATCC TIB-202) were obtained from American Type Culture Collection (Rochville, USA) and maintained in RPMI1640 medium (Sigma Aldrich) supplemented with 10% FCS (Caco-2) and 20% FCS (THP-1), 1% L-glutamine and 1% Pen/Strep (100 U/100 µg/mL). AGS cells

were cultured in RPMI 1640 medium (Sigma-Aldrich) with 2 mM L-glutamine (Biowest) and 10% fetal calf serum (FCS) (Biowest) in a humidified 5% CO₂ atmosphere at 37°C as described.(7) Cells were grown in culture dishes to a confluency of approx. 70%. One hour before infection, medium was replaced with serum free medium (RPMI 1640 medium with 2 mM L-glutamine). Differentiation of THP-1 cells towards macrophage-like cells (THP-1M) was triggered by the addition of PMA (50 ng/mL) for 24 h, followed by a washing step with PBS buffer and the addition of complete media over 48 h post differentiation. For the analysis of cellular infections and for cytotoxicity studies, cells (1x10⁶) were seeded from a confluent culture flask in 35 mm glass bottom dishes (MatTek), 24- or 94-well plates. THP-1 cells were differentiated as previously described and all other cells were cultivated for 24 h. Subsequently, cells were exposed to the respective bacteria suspension (+/- NPs) under standard cell culture conditions. Afterwards, cells were washed three times with PBS buffer to remove the largest part of unattached and non-phagocytosed bacteria. Infected cells were analyzed by different methods of microscopy and PCR. IL-8 in culture supernatants was measured using human IL-8 ELISA (Biolegend) according to manufacturer's instructions.

Immunoblotting. For bacteria NP interaction studies, immunoblotting was carried out as described previously.(2) Antibodies were α -elongation factor thermo unstable (EF-Tu; Hycult biotech, Netherlands) and rabbit- α -mouse IgG Ab conjugated with horseradish peroxidase (Santa Cruz). For *H. pylori* induced CagA phosphorylation, AGS cells were infected with *H. pylori*^{GFP} at a MOI (multiplicity of infection) of 100. After 4 hours of infection, cells were washed twice in PBS, harvested in lysis buffer (20 mM Tris pH 7.5, 100 mM NaCl, 1 % Triton X-100, 0.5 % DOC, 0.1 % SDS, 0.5 % NP-40) and analyzed by immunoblot as described.(7) Briefly, equal amounts of protein were separated by SDS-Page transferred to nitrocellulose membranes and immunoprobed for phospho-tyrosine (pY99, Santa Cruz), total CagA (polyclonal rabbit α -CagA serum) or β -actin (Sigma-Aldrich). Membranes were analyzed with the Odyssey Fc Imaging System (Li-COR Biosciences) using IRdye® 800CW anti-mouse-IgG or IRdye® 700CW anti-rabbit-IgG (Li-COR Biosciences). Band intensities were quantified using ImageStudio (Li-COR Biosciences) and intracellular p-CagA was normalized for β -actin.

Fluorescence Microscopy. Bacteria-nanoparticle interactions and cellular internalization or attachment of bacteria were analyzed by using the AxioVert 200M

microscope (Carl Zeiss,). After the incubation of bacteria and nanoparticles, bacteria were directly given into 35 mm glass bottom dishes (MatTek) for the microscopy of NP-interaction. For the analysis of cellular infections, bacteria-infected cells were fixed with 4 % PFA for 10 min. Cell nuclei were stained with 0.5 µg/mL Hoechst 33342 (excitation: 405 nm; emission: 430-480 nm). Image analysis and presentation were performed as described in detail using the Axiovision software (Carl Zeiss).(2)

Scanning electron microscopy (SEM). All samples were fixed with 2.5 % glutaraldehyde in phosphate buffer 0.1 M under vacuum for 24 h. Bacteria or NP-bacteria complexes were fixed on glass coverslips and examined using a field emission scanning electron microscope (Quanta 200 FEG) as described.(8) To avoid charging up of the samples, images were taken under low vacuum condition (0.9 mbar) with a large field gaseous secondary electron detection system (large field detector). Different magnification levels (10,000x, 50,000x, 100,000x) were used. Beam energy (20 keV) and electron current density (Spot 3) were kept constant for all analyzes. Scanning speed and integration time were selected to avoid beam damages to the bacteria substructures. Image analysis and presentation were performed using the FEI Eindhoven image software (FEI Eindhoven) according to.(8)

AFM. *E. coli* XL2-BlueTM were stained with Bac LightTM Red bacterial stain (Life Technologies) according to manufacturer's protocol. *E.coli* were washed three times with ddH₂O prior to paraformaldehyde fixation for 2 h at RT. After three additional washing steps, the suspension was diluted 1:10 in ddH₂O and 100 µl were transferred onto a microscopy slide which was left to dry over night at RT. For atomic-force microscopy experiments, a JPK instruments BioMAT Workstation was used combining fluorescence microscopy with atomic force microscopy (AFM). The epifluorescence microscope (EFM) consisted of a Zeiss AxioImager.M2.m equipped with a HBO 100 mercury vapor lamp and a 100x air-objective (Zeiss EC Epiplan-NEOFLUAR 100x/0.9 Pol). Images were taken with a digital microscope camera (Zeiss, AxioCam MRm) and processed using Zeiss Zen 2 pro. A JPK instruments NanoWizard II was used as AFM. Images were processed using the JPK SPM Image processing (v.3.x). To combine EFM with AFM, a shuttle stage was applied. The shuttle stage allows an examination of the same spot with both techniques with a spatial deviation of less than 5 µm (Mangold, 2008). Samples were visualized in

intermittent contact mode with a line rate of 0.06 Hz and a tip velocity of 0.5 $\mu\text{m/s}$ using cantilever CSC37, force constant 0.35 N/m (Mikromasch).

Energy Dispersive X-Ray Spectroscopy (EDX). Bacterial samples were fixed with 2.5 % glutaraldehyde. Bacterial surfaces were analyzed by EDX using an INCA 350 Energy spectrometer (Oxford Instrument GmbH) equipped with a PENTAFET Plus Si(Li)-Platinum detection system directly coupled to the Quanta 200 FEG. Spectra were obtained from at highlighted locations with the “Point&ID” mode of the INCA navigation software according to.(8) A minimum of three spectra were taken in the middle of the SEM images with an acquisition time of 60 s each and evaluated with INCA Energy software packages.

Quantification of bacteria internalization in human cells by automated microscopy. To quantify the internalization of bacteria, the automated ArrayScanVTI imaging platform (Thermo Fisher Scientific Inc.) was used as described previously.(2) Cells were seeded with an electronic multichannel pipette (Eppendorf) into 24-well cell culture plates (Greiner) and incubated in a 5% CO_2 humidified atmosphere at 37 °C. Cells were infected with different bacteria suspensions (+/- NPs) for 90 min under standard cell culture conditions. After washing with PBS buffer for three times, cells were fixed with 4% PFA for 10 min and the nuclei were stained with 0.5 $\mu\text{g/mL}$ Hoechst 33342 (excitation: 405 nm; emission: 430-480 nm). Images were analyzed using the SpotDetection assay. Briefly, for every cell, a binary image mask was created from the Hoechst staining signal (XF100 Hoechst 355/465) to define the region of interest. In the second channel (XF93 GFP 475/515), this circular mask was dilated (two pixels) to cover the whole cell and the spot number of the fluorescent bacteria was quantified within this mask. Scans were performed sequentially with settings to give sub-saturating fluorescence intensity. A minimum of 1,500 cells/well was recorded. PBS- and medium-treated cells served as a negative control to correct for background fluorescence. Each experiment was performed in triplicates.

PCR. DNA of infected blood was isolated using the DNeasy Blood and Tissue Kit (Qiagen). The DNA concentration was measured with the Nanodrop-2000 (Thermo Fisher Scientific). PCR analysis was performed using the Phusion Blood Direct PCR Kit (Thermo Scientific). A typical PCR sample consisted of a 25- μL volume containing 0.5 μM of the

primers (pGEX-GFP-for 5'- AAA CGA GGA GCT GTT CAC CGG -3'; pGEX- GFP-rev 5'-
TTT CCA TGC CGT GAG TGA TGC C -3'), 1X Phusion Blood PCR buffer, 1X Phusion
Blood II DNA Polymerase and 200 ng DNA of the respective sample. The following PCR
5 conditions were applied: 5 min, 98 °C initial denaturation; 1 s, 95 °C cyclic denaturation;
30 s, 72 °C cyclic extension for a total of 35 cycles, followed by 1 min, 72 °C final
extension (protocol provided by Thermo Scientific). PCR amplification products were
mixed with 1X DNA loading dye (xylene cyanol) and separated on a 1% agarose gel with
0.3x10⁻³% ethidium bromide. Gels were run at the constant voltage of 75 V for 60 min, and
the separation was documented with the transilluminator Multigenius Bioimagine
10 (Syngene) at 260 nm.

Human Tissue Material. Human corpus tissue was obtained from 17 patients (12 men,
5 women; age range, 41–87 y) who underwent partial or total gastrectomy at the
University Medical Centre Utrecht. Ten patients were diagnosed with gastric cancer and 7
15 patients were diagnosed with esophageal cancer. This study was approved by the ethical
committee of the University Medical Centre Utrecht. Samples were obtained with informed
consent.(9)

Organoid culture and infection. Glands were extracted from 1 cm² of human tissue
20 using EDTA in cold chelation buffer(10) seeded in Matrigel (BD Biosciences), and overlaid
with medium containing advanced Dulbecco's modified Eagle medium (DMEM)/F12
supplemented with penicillin/streptomycin, 10 mmol/L HEPES, GlutaMAX, 1 B27 (all from
Invitrogen), and 1 mmol/L N-acetylcysteine (Sigma-Aldrich). Growth factors were added to
the basal medium as indicated in.(9) The final human stomach culture medium contained
25 the following essential components: 50 ng/mL epidermal growth factor (EGF) (Invitrogen),
10% noggin-conditioned medium, 10% R-spondin1-conditioned medium, 50% Wnt-
conditioned medium, 200 ng/mL fibroblast growth factor (FGF)10 (Peprotech), 1 nmol/L
gastrin (Tocris), and 2 mmol/L transforming growth factor (TGF)bi (A-83-01; Tocris). The
facultative component was 10 mmol/L nicotinamide (Sigma-Aldrich). After seeding, 10
30 mmol/L rho-associated coiled coil forming protein serine/threonine kinase (RHOK) (Y-
27632; Sigma-Aldrich) was added. Additional tested components were as follows: 100
ng/mL insulin-like growth factor (IGF) (Peprotech), 10 mmol/L p38 inhibitor (SB202190;
Sigma-Aldrich), 3 mmol/L glykogensynthase-Kinase (GSK)3b inhibitor (CHIR99021; Axon
Medchem), and 500 nmol/L prostaglandin E (PGE)2 (Tocris). Approximately 1 cm² of

cancer tissue was cut into small fragments and washed in cold chelation buffer until the supernatant was clear. Fragments were subjected to enzymatic digestion by 1.5 mg/mL collagenase (Gibco) and 20 mg/mL hyaluronidase (Sigma-Aldrich) in 10 mL advanced DMEM/F12 (Gibco), supplemented with antibiotics (Primocin; Invivogen), for 1 hour at 37 °C with shaking. Cells were washed twice in advanced DMEM/F12, seeded into Matrigel, and overlaid with medium containing HEPES, GlutaMAX, penicillin, streptomycin, B27, n-acetylcysteine, EGF, Rspodin1, noggin, Wnt, FGF10, gastrin, TGFb inhibitor, and RHOK inhibitor as described.(9)

Organoids were microinjected on day 10 after seeding with an approximate multiplicity of infection (MOI) of 50 unless otherwise stated. For calculation of MOI, organoids were disrupted into single cells by EDTA and cells were counted (approximately 4000 cells/organoid). To achieve a final MOI of 50, pristine *H. pylori*^{GFP} and *H. pylori*^{GFP} pre-incubated with NPs as described earlier were suspended in advanced DMEM/F12 at a density of 1x10⁹/mL and organoids were injected with approximately 0.2 µL bacterial suspension using a micromanipulator and microinjector (M-152 and IM-5B; Narishige) under a stereomicroscope (MZ75; Leica) inside a sterile bench (CleanAir). Images were taken using standard or confocal microscopy (Eclipse E600; Nikon, Chiyoda, Japan; or DMIL or SP5; Leica). Images were taken on a Nikon Eclipse E600.

Reagents. Standard reagents were purchased from Sigma Aldrich. Fetal calf serum (FCS) was purchased from Gibco, Life Technologies GmbH.

Statistical Analysis. For experiments stating p values, a paired Student's t-test was performed as described previously,(5) assuming significance at *P,0.05; **P,0.01; ***P,0.005.

SUPPLEMENTARY TABLES

Supplementary Table S1 EDX analysis.						
Samples	C	N	O	Na	Si	Ce
<i>H. pylori</i>	64.11	12.06	21.73	1.01	0	0
<i>H. pylori</i> + Si ₃₀	50.43	9.62	34.99	0.28	3.98	0

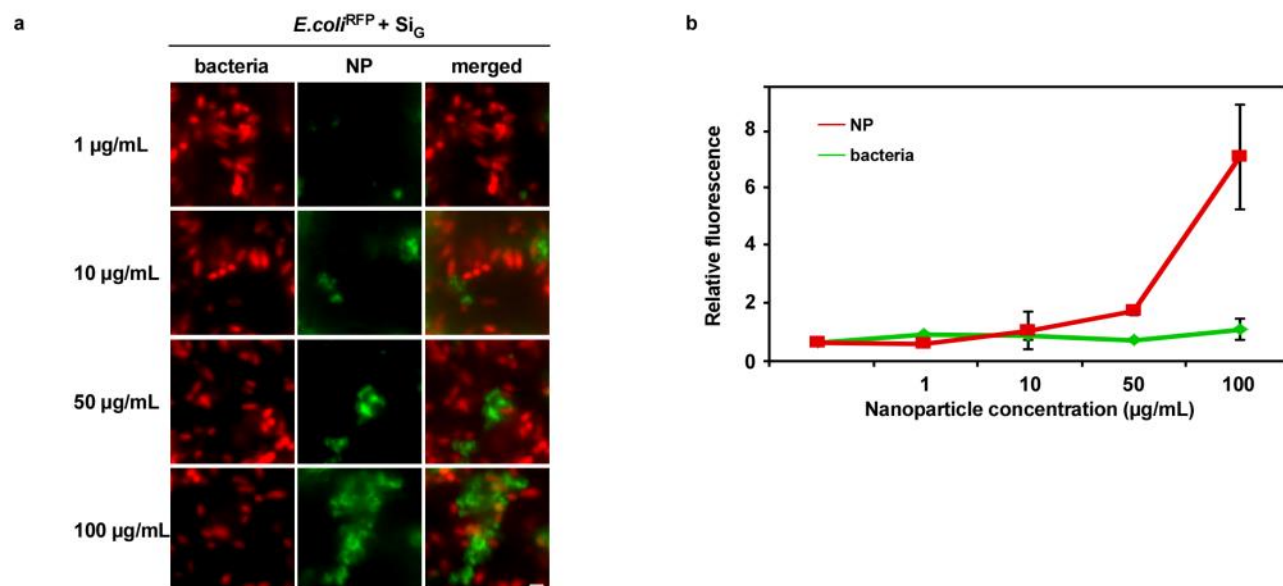
5 **Supplementary Table S1. EDX analysis.** Si was only detected in the sample treated with Si₃₀. Numbers are given in atomic percent.

Supplementary Table S2 Gastric fluid (GF) simulation media	
Components	GF
Pepsin	0.1 mg/mL
Sodium taurocholate	80 μM
Lecithin	20 μM
Sodium chloride	34.2 mM
Orthophosphoric acid	-
Sodium dihydrogenphosphate	-
Milk/buffer	1:1
Hydrochloric acid	for GF pH 3

10 **Supplementary Table S2. Gastric fluid (GF) simulation media.** Gastric fluid was used to simulate gastric conditions.

SUPPLEMENTARY FIGURES

Supplementary Fig. S1

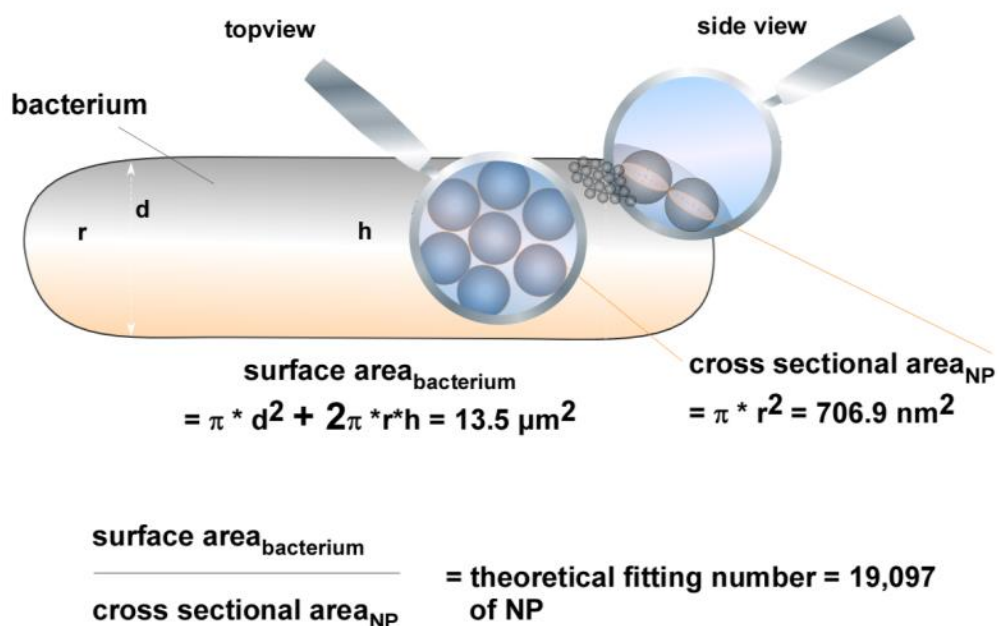
**Supplementary Figure S1| Investigation of NP-bacteria complex formation.**

5 Increasing amount of NPs results in higher numbers of NP-bacteria complexes *in situ*. Representative images of NP-bacteria complexes visualized by fluorescence microscopy. Scale bars, 2 μm . **b**, Quantification of NP-bacteria interaction using the ArrayScanVTI automated microscopy platform. 1×10^6 red fluorescent bacteria were incubated with the indicated concentrations of green fluorescent NPs, and complexes analyzed in 96-well plates. A minimum of 1,000 NP-bacteria complexes/well was analyzed for green and red fluorescence in triplicates using the TargetActivation assay. Increasing concentrations of NPs resulted in increased binding to bacteria. Red and green fluorescence intensity of complexes is displayed. As a control, the signal of GFP-expressing bacteria remains constant.

10

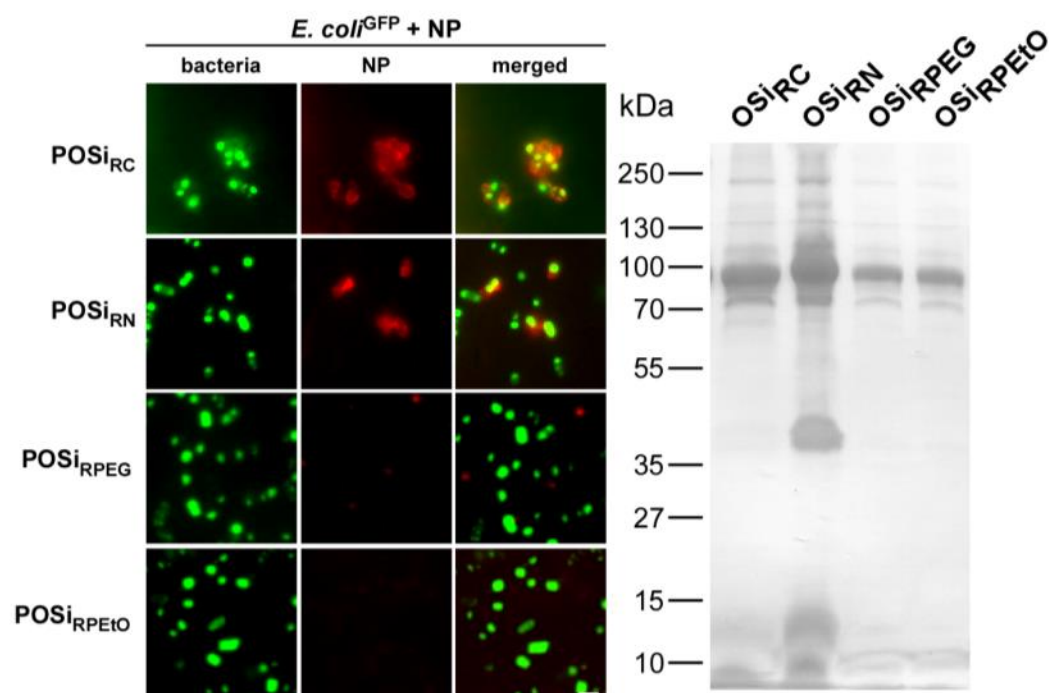
15

Supplementary Fig. S2



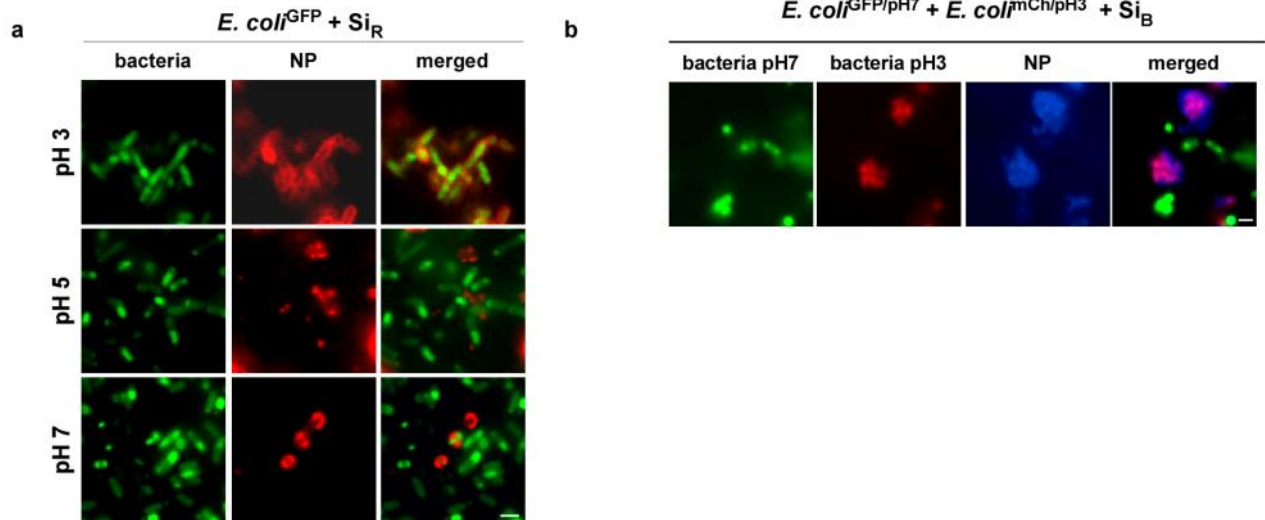
Supplementary Figure S2| Calculation of maximal surface occupation by NPs. The surface area of a single bacterium is $\sim 13.5 \mu\text{m}^2$. The maximum area occupied by NPs (Si₃₀; $\varnothing \sim 30 \text{ nm}$) corresponds to their cross sectional area of $\sim 706.9 \text{ nm}^2$. Hence, it is estimated that maximally $\sim 2 \times 10^4$ NP can bind to a single bacterium. Objects not drawn to scale. **g**, Fluorescence-based automated quantification of complex formation revealed no significantly improved binding for less negatively charged Si NPs (Table 1). Data are representatives of two independent experiments.

Supplementary Fig. S3



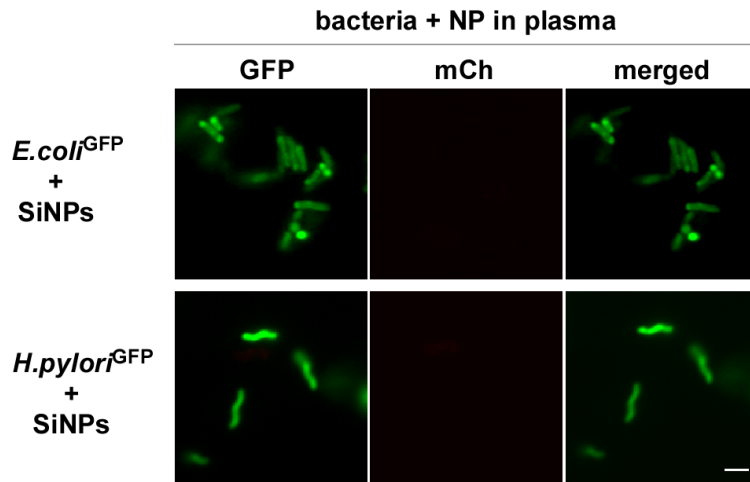
Supplementary Figure S3| Physico-chemical characteristics of NPs are critical for complex formation with bacteria. Positively- (POSi_{RN}) and negatively- (POSi_{RC}) charged poly(organosiloxane) NPs bound to bacteria whereas less binding was observed for the negatively charged NPs and no binding occurred for 'stealth'-modified NPs. All images are representatives of three independent experiments. (Left panel) SDS-PAGE demonstrates reduced overall plasma protein binding for 'stealth'-modified NPs by the addition of poly(ethylene glycol) or poly(2-ethyl-2-oxazoline). NPs were incubated in undiluted human plasma for 30 min and washed. (Right panel)

Supplementary Fig. S4



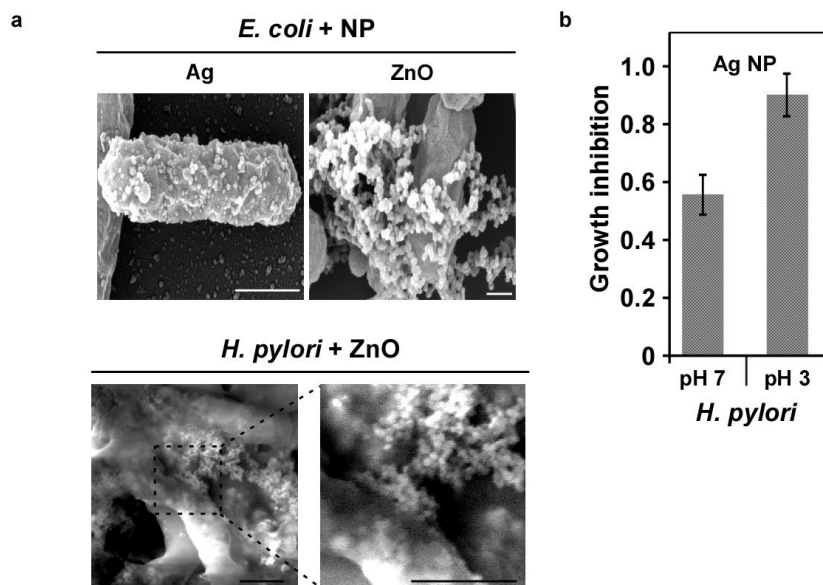
Supplementary Figure S4| NP-bacteria complex formation is pH-dependently enhanced. **a**, Bacteria were incubated with Si_R at the indicated pH for 10 min. NP-bacteria complex formation increased with lowering the pH. **b**, When bacteria, pre-treated at pH 3, were mixed with bacteria, pre-treated at pH 7, and exposed to NPs at pH 7, NPs preferentially assembled on pH 3-treated pathogens. Scale bars 2 μm.

Supplementary Fig. S5



Supplementary Figure S5| Impact of the biomolecule corona on NP-bacteria complex formation. The plasma biomolecule corona reduces NP-bacteria complex formation. Green fluorescent pathogens were incubated with red fluorescence Si in the presence of human plasma and analyzed by fluorescent microscopy. Scale bars 2 μ m.

Supplementary Figure 6

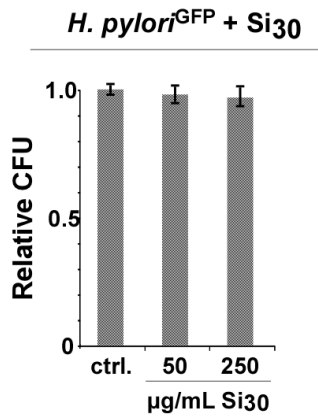


Supplementary Figure S6| Enhanced binding of NPs to bacteria improves the antibacterial activity of the NPs.

5 NPs. Scale bar 2 μm . **b**, pH-dependent enhancement of NP-bacteria complex formation increases Ag NPs' antibacterial activity. Bacteria were incubated with Ag NPs (50 $\mu\text{g}/\text{mL}$) in PBS at pH 7 or 3. After washing, NP-bacteria complexes were cultured and growth inhibition determined, using optical density at 6 h. Growth inhibition defined as: $1 - (\text{OD}_{\text{NP}} / \text{OD}_{\text{ctrl}})$. Values above 0 indicate antibiotic effects. Columns show the mean \pm s.d. from

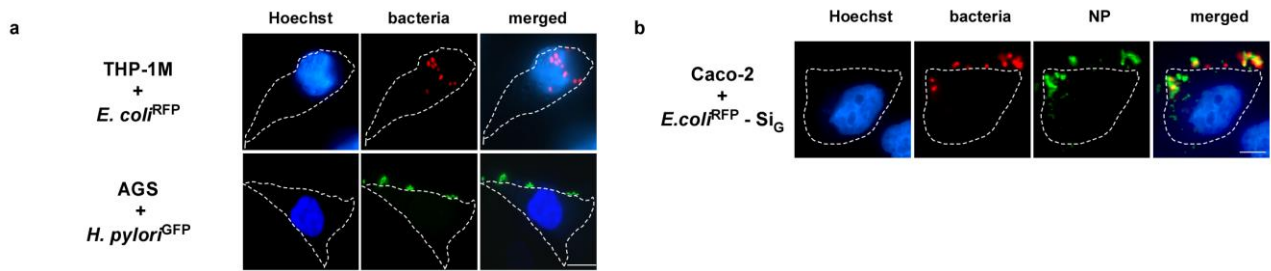
10 three independent experiments.

Supplementary Fig. S7



Supplementary Figure S7| Bacterial viability was not affected by Si₃₀ even when high concentrations were used. CFU assays of *H. pylori* 24 h after exposure to the indicated Si₃₀ concentrations.

Supplementary Fig. S8



Supplementary Figure S8| Impact of NP-pathogen complex formation. **a**, Attachment and uptake of bacteria in human cells. THP-1M macrophages or AGS gastric epithelial cells were exposed to the indicated bacteria. **b**, Attachment and uptake of NP-bacteria complexes in Caco-2 cells. Scale bars 10 μ m. Images are representatives of three independent experiments. Scale bars 10 μ m

Supplementary References

1. Docter D, Distler U, Storck W, Kuharev J, Wunsch D, Hahlbrock A, et al. Quantitative profiling of the protein coronas that form around nanoparticles. *Nature protocols*. 2014;9(9):2030-44. 5
2. Tenzer S, Docter D, Kuharev J, Musyanovych A, Fetz V, Hecht R, et al. Rapid formation of plasma protein corona critically affects nanoparticle pathophysiology. *Nature nanotechnology*. 2013;8(10):772-81.
3. Xiao J, Kuc A, Pokhrel S, Madler L, Pottgen R, Winter F, et al. Fe-doped ZnO nanoparticles: the oxidation number and local charge on iron, studied by ⁵⁷Fe Mossbauer spectroscopy and DFT calculations. *Chemistry*. 2013;19(10):3287-91. 10
4. Koshkina O, Westmeier D, Lang T, Bantz C, Hahlbrock A, Wurth C, et al. Tuning the Surface of Nanoparticles: Impact of Poly(2-ethyl-2-oxazoline) on Protein Adsorption in Serum and Cellular Uptake. *Macromol Biosci*. 2016.
5. Tenzer S, Docter D, Rosfa S, Wlodarski A, Kuharev J, Rekić A, et al. Nanoparticle Size Is a Critical Physicochemical Determinant of the Human Blood Plasma Corona: A Comprehensive Quantitative Proteomic Analysis. *ACS nano*. 2011;5(9):7155-67. 15
6. Schmitt W, Haas R. Genetic analysis of the *Helicobacter pylori* vacuolating cytotoxin: structural similarities with the IgA protease type of exported protein. *Mol Microbiol*. 1994;12(2):307-19. 20
7. Krisch LM, Posselt G, Hammerl P, Wessler S. CagA Phosphorylation in *Helicobacter pylori*-Infected B Cells Is Mediated by the Nonreceptor Tyrosine Kinases of the Src and Abl Families. *Infect Immun*. 2016;84(9):2671-80.
8. Ritz U, Gotz H, Baranowski A, Heid F, Rommens PM, Hofmann A. Influence of different calcium phosphate ceramics on growth and differentiation of cells in osteoblast-endothelial co-cultures. *J Biomed Mater Res B Appl Biomater*. 2016. 25
9. Bartfeld S, Bayram T, van de Wetering M, Huch M, Begthel H, Kujala P, et al. In vitro expansion of human gastric epithelial stem cells and their responses to bacterial infection. *Gastroenterology*. 2015;148(1):126-36 e6.
10. Sato T, Stange DE, Ferrante M, Vries RG, Van Es JH, Van den Brink S, et al. Long-term expansion of epithelial organoids from human colon, adenoma, adenocarcinoma, and Barrett's epithelium. *Gastroenterology*. 2011;141(5):1762-72. 30